Fission-Track Dating of Haughton Astrobleme and Included Biota, Devon Island, Canada

GOMAA OMAR, KIRK R. JOHNSON, LEO J. HICKEY, P. BLYTH ROBERTSON, MARY R. DAWSON, CATHY W. BARNOSKY

Haughton Astrobleme is a major extraterrestrial impact structure located on Devon Island in the Canadian Arctic Archipelago, Northwest Territories. Apatite grains separated from shocked Precambrian gneiss contained in a polymict breccia from the center of the astrobleme yielded a fission-track date of 22.4 million ± 1.4 million years before the present or early Miocene (Aquitanian). This provides a date for the impact event and an upper limit on the age of crater-filling lake sediments and a flora and vertebrate fauna occurring in them. A geologically precise date for these fossils provides an important biostratigraphic reference point for interpreting the biotic evolution of the Arctic.

HAUGHTON ASTROBLEME LIES IN the north central portion of Devon Island in the Canadian Arctic Archipelago (75°22′N, 89°40′W) (Fig. 1). It is a circular, multiring structure, some 20 km in diameter, with a relatively subtle topographic expression, and is superimposed on a gently west-dipping, 1700-m sequence of early Paleozoic limestone, dolomitic shale, and gypsum unconformably overlying the crystalline Precambrian basement (*1*). Shatter cones (*2*), microscopic shock-metamorphism in clasts in polymict allochthonous breccia, and a number of large-scale structural features, such as annular faulting (*3*), all point to the structure's origin by hypervelocity impact and conform to the definition of "astrobleme," a terrestrial feature inferred to be the result of impact by a cosmic body (*4*).

Although the polymict breccia is overwhelmingly dominated by carbonate clasts, it also contains rare but ubiquitous clasts of Precambrian basement gneiss, with locally higher concentrations near the structure's center and at the northeast corner of the inner ring. There are no outcrops of the gneiss exposed anywhere in the vicinity of the astrobleme.

A 48-m thick sequence of cyclically bedded, dolomitic silt and mudstone overlies the impact breccia and represents the sediments of a crater-filling lake (*5*). These sediments have yielded a fauna including fishes (smelt and trout), a primitive rhinocerotid, a soricid, a primitive leporid, and a pecoran artiodactyl with a highly derived tooth pattern. Fossil plants are represented by a pollen flora dominated by *Pinus, Picea, Betula, Alnus*, and *Corylus*-type pollen with lesser amounts of *Tsuga, Larix, Ulmus/Zelkova, Carva, Ostrya/Carpinus*, Ericaceae, *Juglans*, and trace occurrences of *Liquidambar* and *Castanea*; a megaflora composed of fruits and seeds of numerous as yet unidentified angiosperms, as well as cones and needles of *Larix, Pinus*, and *Picea*, and a single leaf of *Betula*. Extreme geographic isolation from correlative assemblages and lack of index fossils previously made it impossible to determine a more precise age than mid-Tertiary (20 million ± 5 million years ago) for the Haughton biota (*1, 5, 6*). A somewhat similar but apparently cooler flora from the Beaufort Formation extending from Meighen to Banks Island has been dated by paleobotanical correlation as Miocene to Pliocene (*7, 8*).

Nearly 40 kg of loose gneiss clasts were collected from the surface of smoothly weathering breccia slopes 3 km northwest of the crater's geometric center (G, Fig. 1). These clasts were easily recognized in the field by their low density. Apatite grains were recovered from these clast samples by conventional heavy liquid and magnetic separation methods. No zircon or sphene (minerals commonly used in fission-track analysis) were recovered from these rocks. Preparation of the apatite for fission-track dating using the external detector method followed procedures described by Naeser (*9*), where muscovite detectors (geometry factor 0.5) were used.

Two separate irradiations were performed on the same apatite mounts at the thermal neutron facility (RT-4) of the National Bureau of Standards (NBS) research reactor at Gaithersburg, Maryland. Apatite mounts and mica detectors were etched in 5*N*

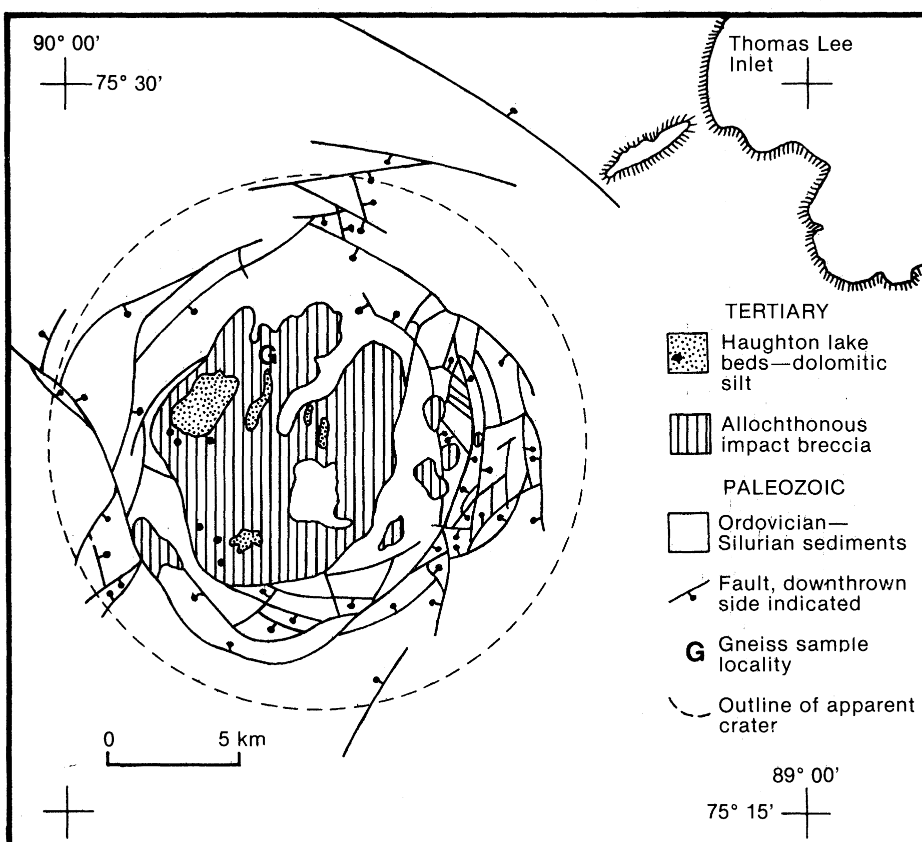

Fig. 1. Generalized geology of Haughton Astrobleme (*3*) showing the outline of the apparent crater, pattern of faulting, distribution of the Tertiary lake beds and the impact breccia as well as the location of the gneiss samples used in the fission-track dating of the impact.

G. Omar, Department of Geology, University of Pennsylvania, Philadelphia, PA 19104.
K. R. Johnson and L. J. Hickey, Department of Geology and Geophysics, Yale University, New Haven, CT 06511.
P. B. Robertson, Geological Survey of Canada, Ottawa, Ontario, Canada K1A 0Y3.
M. R. Dawson and C. W. Barnosky, Carnegie Museum of Natural History, Pittsburgh, PA 15213.

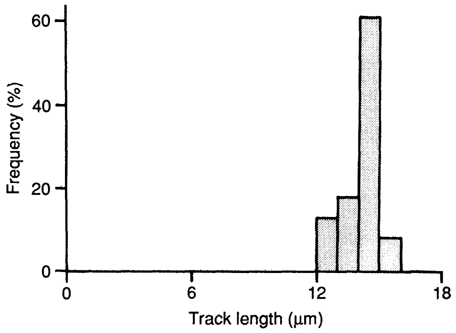

Fig. 2. Fission-track length distribution in apatite for preexistent tracks from Haughton Astrobleme. Mean track length ± standard error, 14.2 ± 1.1 μm; standard deviation, 0.79 μm; number of tracks measured, 53.

HNO_3 for 25 seconds at 22°C. Mica detectors covering apatite mounts and glass standards were etched in 48% HF for 25 and 45 minutes, respectively, at 22°C. The lengths of horizontal confined (fully etched and totally embedded in the mineral) fission tracks were measured with a dry objective at a magnification of ×1250.

Neutron doses were determined by counting tracks in muscovite detectors in contact with SRM-614 standard glass during irradiations. Ages were calculated using the NBS-963a copper calibration for neutron fluence (*10*) with $\lambda_F = 7.03 \times 10^{-17}$ year^{-1}. This value of λ_F together with the neutron doses determined from the two irradiations performed for this study, yielded ages of 27.1 million ± 2.4 million (11 grains) and 28.6 million ± 2.3 million years old (10 grains) for the Fish Canyon Tuff apatite age standard from Colorado, whose standard K-Ar date based on sanidine, hornblende, biotite, and plagioclase is 27.79 million ± 0.14 million years old (*11*). The close agreement of the fission-track ages and K-Ar ages of the age standard indicate that with $\lambda_F = 7.03 \times 10^{-17}$ year^{-1} the NBS-963a copper calibration values for the neutron doses represent a good empirical calibration of the fission-track ages to the K-Ar method (*12*).

Uncertainty in the age of each sample was evaluated by applying the chi-square test (at the 5% level) to check the variance of individual grain ages within the sample against the variance expected from an age-homogeneous sample with only Poisson counting error (Table 1). The uncertainties of the ages were determined by taking into account the uncertainties in the pre-existent, induced, and neutron-dose dosimetry track counts following the procedure described by Green (*13*). The fission-track analytical data and calculated ages for apatite from the Haughton impact crater are shown in Table 1 and Fig. 2.

The mineral apatite has been used to date meteorite impacts by the fission-track method (*14*). However, this technique will yield the correct impact age only if all pre-impact fission tracks were erased either by the intense thermo-barometric effects of the shock wave itself (*15*) or by the residual heat of the impact retained primarily in melts and in thick deposits of allochthonous breccia (*16*). Shock waves that create pressures greater than 40 GPa are known to totally erase fission tracks in apatite (*15*).

Haughton gneiss clasts exhibit shock metamorphism ranging from partial isotropization of tectosilicate minerals (~25 GPa) to the development of a highly vesicular, largely homogenized mixture of glassy quartz and feldspars, with distinctive flow textures (~60 GPa). Most, however, including those from which apatite was extracted for this analysis, exhibit shock metamorphism indicative of pressures in the 40- to 50-GPa range. Quartz is diaplectic, with as much as 10% conversion to coesite along irregular fractures. Feldspars are completely glassy, ranging from diaplectic grains to a glassy continuum containing immiscible globules, flow textures, and incipient to extensive vesiculation. Unresolvable, irregular mafic concentrations represent dissociation products of biotite and amphibole. Sillimanite remains birefringent and displays planar features and thermal erosion at the margins.

Stöffler (*17*) compiled instantaneous shock temperatures and prolonged, post-shock temperatures in quartz and feldspars, as a function of shock level in a large-scale impact event. Post-shock temperatures for quartz and plagioclase (glasses) in the 40- to 50-GPa range would be 500° to 1150°C and 400° to 800°C, respectively. Although comparable data for apatite were not compiled, the post-shock thermal environment of the Haughton gneiss clasts would have been dominated by the abundant quartz and feldspar, so that localized, immediate, post-shock temperatures in the rare and small apatite grains would soon have been overridden by the tectosilicate thermal regime. It is almost certain, therefore, that apatites selected for this study have experienced prolonged temperatures of at least 400°C, and probably as high as 800° to 1000°C. In comparison, a temperature estimated at 360°C for 1 hour completely erased preexisting tracks in apatite from the Ries Astrobleme (*16*). Thus, we have assumed that all preimpact tracks in the apatite grains dated here were erased.

Conversely, reduction in apparent age through thermal annealing of tracks that developed in the apatite grains subsequent to impact could have occurred in a thermal regime between 70° and 125°C that persisted for times on the order of 10^7 years (*18, 19*). Assuming a moderate geothermal gradient, this would have required 2 to 3 km of sedimentary cover, a depth well in excess of that suggested by sedimentary or other evidence at the site.

Furthermore, the length distribution of horizontal "confined" tracks clearly shows that annealing has not occurred. When first formed, tracks in apatite show a narrow distribution with a mean track length of 16.3 ± 0.9 μm (*20, 21*). Preexistent fossil tracks, however, are always shorter than freshly formed ones, even for samples with a simple, rapid cooling history. This is the case for fission tracks in apatite from the Fish Canyon Tuff where a 6% shortening is observed (*22*). Nevertheless, Gleadow and Duddy (*19*) observed that a shortening of up to 20% can occur in apatites before any reduction in fission-track age is noted. Thus, the Fish Canyon Tuff apatite fission-track ages (*23*) are concordant with K-Ar ages of other minerals present in the same rock (*11*). Apatite from the Haughton Astrobleme showed a 13% reduction in the mean length of preexistent tracks compared to the mean length of freshly formed tracks (Fig. 2). This is significantly less shortening than is required for track density and thus fission-track age to be reduced. For these reasons we conclude that the apatite fission-track age of 22.4 million ± 1.4 million years is the date of the hypervelocity impact event which formed Haughton Astrobleme.

Table 1. Apatite fission-track analytical results and ages of shocked crystalline rocks from Haughton Astrobleme.

Sample	ρ_s* × 10^6 (tracks/cm^2)	ρ_i† × 10^6 (tracks/cm^2)	ϕ‡ × 10^{15} (neutrons/cm^2)	Grains counted (No.)	Test of variance	Age ± 1σ (×10^9 years)
			First irradiation			
HUA-855	0.80 (505)§	13.86 (4401)	6.28 (3171)	11	Passed	21.7 ± 1.2
			Second irradiation			
HUA-855	0.69 (452)	16.89 (5552)	9.44 (2085)	10	Passed	23.0 ± 1.2
					Average	22.4 ± 1.4

*ρ_s = spontaneous track density. †ρ_i = induced track density. ‡ϕ = thermal neutron dose. §Values in parentheses are the number of tracks counted.

Our field evidence for rapid onset of lacustrine deposition after impact (*24*) and the relatively rapid rates of accumulation recorded for such sediments (*25*) allow us to fix the date for the Haughton fossil assemblages well within the limit of error for our fission-track values. This provides an invaluable datum point for the hitherto poorly dated Neogene plant assemblages of the Arctic that will be of considerable importance for understanding paleogeography and biostratigraphy of the region during that time.

REFERENCES AND NOTES

1. T. Frisch and R. Thorsteinsson, *Arctic* **31**, 108 (1978).
2. P. B. Robertson and G. D. Mason, *Nature (London)* **255**, 393 (1975).
3. P. B. Robertson and J. F. Sweeney, *Can. J. Earth Sci.* **20**, 1134 (1983).
4. American Geological Institute, *Dictionary of Geological Terms* (Anchor/Doubleday, Garden City, NY, 1976).
5. P. B. Robertson *et al.*, *Proc. Lunar Planet Sci. Conf. 16th* (1985), p. 702.
6. M. R. Dawson *et al.*, *Can. Paleontol. Biostratigr. Sem. Quebec* (1985), p. 8.
7. L. V. Hills, in *Proceedings of the Circumpolar Conference on Northern Ecology*, (National Research Council Canada, Ottawa, 1975), p. I-65.
8. J. V. Matthews, *Geol. Surv. Can. Pap.* **87-1A**, 73 (1987).
9. C. W. Naeser, *U.S. Geol. Surv. Open-file Rep. 76-190* (1978).
10. B. S. Carpenter, *Natl. Bur. Stan. Spec. Publ. 260-292* (1984).
11. M. J. Kunk, J. F. Sutter, C. W. Naeser, *Geol. Soc. Am. Abstr. Programs* 17, 636 (1985).
12. Dates were calculated from the age equation of R. L. Fleischer, P. B. Price, and R. M. Walker [*Nuclear Tracks in Solids: Principles and Applications* (Univ. of California Press, Berkeley, 1975)]. The constants used for age calculations are: $\lambda_D = 1.551 \times 10^{-10}$ year^{-1}, $^{235}U/^{238}U = 7.252 \times 10^{-3}$; and $\sigma^{235} = 580.2 \times 10^{-24}$ cm^2.
13. P. F. Green, *Nucl. Tracks* **5**, 77 (1981).
14. D. Storzer and G. A. Wagner, *Meteoritics* **12**, 368 (1977).
15. R. L. Fleischer, R. T. Wood, H. R. Hart, Jr., P. B. Price, N. M. Short, *J. Geophys. Res.* **79**, 339 (1974).
16. D. S. Miller and G. A. Wagner, *Earth Planet. Sci. Lett.* **43**, 351 (1979).
17. D. Stöffler, *J. Geophys. Res.* **76**, 5541 (1971).
18. C. W. Naeser, *Nucl. Tracks* **5**, 248 (1981).
19. A. J. W. Gleadow and I. R. Duddy, *ibid.*, p. 169.
20. A. J. W. Gleadow, I. R. Duddy, J. F. Lovering, *Aust. Pet. Explor. Assoc. J.* **23**, 93 (1983).
21. K. D. Crowley, C. W. Naeser, C. A. Babel, *Earth Planet Sci. Lett.* **79**, 329 (1986).
22. R. K. Dokka *et al.*, *Tectonics* **5**, 995 (1986).
23. C. W. Naeser, R. A. Zimmerman, G. T. Cebula, *Nucl. Tracks* **5**, 65 (1981).
24. This evidence includes the following features of the lacustrine sediments: a reverse-graded debris flow in the basal 2 m; the general lack of reworking or of primary depositional features; and the gradational contact with the underlying ejecta blanket.
25. At minimum rates of lacustrine sedimentation [D. E. Schindel, *Paleobiology* **6**, 425 (1980)] the maximum time to accumulate the 48 m of these sediments is 4.8×10^5 years.

26. We gratefully acknowledge comments by T. Lutz, R. Shagam, and R. Giegengack; S. Carpenter irradiated the samples; and A. Kelly and B. Tiffney identified the fruit and seed remains. Funding for fieldwork was provided by the National Geographic Society and the Polar Continental Shelf Project, Department of Energy, Mines and Resources of the Canadian Government. This is contribution 15287 of the Geological Survey of Canada.

20 April 1987; accepted 27 July 1987

An in Vitro Neurite-Promoting Antigen Functions in Axonal Regeneration in Vivo

ALFRED W. SANDROCK, JR. AND WILLIAM D. MATTHEW*

The function of the neurite growth–promoting antigen INO has been tested in an in vivo neurite regeneration system, the rat iris. The sympathetic innervation of the irides was removed by a single systemic injection of 6-hydroxydopamine. The subsequent regeneration of sympathetic axons into the iris of one eye bathed by the INO antibody, which inhibits neurite growth in vitro, was compared with the regrowth of sympathetic axons into the iris of the animal's other eye, which contained control antibody. Antibodies were released within the eye by implanted hybridoma cells. Neurite regeneration was measured by assaying [^{3}H]norepinephrine uptake into freshly explanted irides. The blockage of the function of the INO antigen by the antibody resulted in a decreased rate of axonal regeneration, thus suggesting the involvement of the INO antigen in the process of neurite regeneration in vivo.

IN THIS REPORT WE PRESENT EXPERImental evidence for the role of the neurite growth–promoting INO antigen in the regeneration of sympathetic nerve fibers in vivo. The INO antibody, which was generated to the neurite promoting activity found in non-neuronal cell conditioned media, recognizes a laminin–heparin sulfate proteoglycan complex (*1*) and inhibits the in vitro neurite growth of sympathetic neurons over cryostat sections of sciatic nerve (*2*). To test the possible function of the INO antigen in vivo, regenerating axons were exposed to the INO antibody by injecting hybridoma cells into the anterior chamber of rat eyes. Treatment with 6-hydroxydopamine (6-OHDA) caused degeneration of sympathetic terminals in the irides; subsequent regeneration, in the presence of three different hybridomas that secreted immunoglobulin M (IgM) monoclonal antibodies, was assayed by explanting irides into culture media containing radiolabeled norepinephrine.

The iris is innervated by sympathetic fibers from the superior cervical ganglion, by parasympathetic fibers from the ciliary ganglion, and by sensory fibers from the trigeminal ganglion (*3*). The axons, in association with Schwann cells (*4*), enter the iris at the ciliary margin, course radially toward the pupil in the stroma, forming a "ground plexus," which lacks Schwann cells (*4*). The sympathetic innervation of the iris can be selectively lesioned by systemic administration of high doses of 6-OHDA, a catecholamine congener, which causes the degeneration of preterminal and terminal axons (*5*–*7*). Because neuronal cell bodies survive 6-OHDA administration in adults (*6*), sympathetic axons begin to regenerate soon after this chemical sympathectomy; complete return of the sympathetic ground plexus to peripheral organs is usually achieved after about 2 months (*8*). The regeneration of sympathetic nerve fibers has been monitored by the return of norepinephrine content (*7*) and high-affinity norepinephrine uptake (*9*) in peripheral organs; the recovery of these biochemical properties parallels the density of catecholamine histofluorescent axons.

The iris separates the anterior and posterior chambers of the eye and is bathed in aqueous humor. A "blood-aqueous barrier" limits exchange of materials between the blood and the aqueous humor of the eye (*10*) and at least partially protects the chambers from immune surveillance (*11*). Mouse hybridoma cells can grow in the anterior chamber and provide a continuous, long-

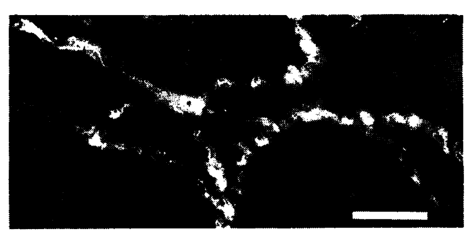

Fig. 1. Localization of the INO antigen in an iris whole mount. Irides were removed from killed animals and placed in 2% paraformaldehyde in 0.1*M* phosphate buffer, *p*H 7.4. After a 15-minute incubation at room temperature, the fixative was removed with three 10-minute rinses of L15 medium containing 10% fetal calf serum. The irides were incubated in 3 ml of hybridoma supernatant for 24 hours at 4°C. After three 1-hour rinses with PBS at room temperature, the irides were rinsed for an additional 24 hours with PBS at 4°C. The irides were incubated in 2 ml of fluorescein-conjugated goat antiserum to mouse immunoglobulins (1:50 dilution in PBS containing 10% rat serum; Antibodies, Inc.). After a 4-hour incubation at room temperature, the irides were rinsed with three 1-hour rinses of PBS at room temperature, gently stretched (stroma side up) on a glass slide and mounted in a 50:50 (v/v) mixture of glycerol and *p*-phenylenediamine (1 mg/ml) in 0.1*M* carbonate buffer, *p*H 8.3. Scale bar, 50 μm.

Department of Neurobiology, Harvard Medical School, 25 Shattuck Street, Boston, MA 02115.

*To whom correspondence should be addressed.